

Contact angles of a drop pinned on an incline

Joël De Coninck

Laboratoire de Physique des Surfaces et Interfaces
Université de Mons, 20 Place du Parc, 7000 Mons, Belgium

François Dunlop and Thierry Huillet

Laboratoire de Physique Théorique et Modélisation, CNRS-UMR 8089
Université de Cergy-Pontoise, 95302 Cergy-Pontoise, France

For a drop on an incline with small tilt angle α , when the contact line is a circle of radius r , we derive the relation $mg \sin \alpha = \gamma r \frac{\pi}{2} (\cos \theta^{\min} - \cos \theta^{\max})$ at first order in α , where θ^{\min} and θ^{\max} are the contact angles at the back and at the front, m is the mass of the drop and γ the surface tension of the liquid. We also derive the same relation at first order in the Bond number $B = \rho g R^2 / \gamma$, where R is the radius of the spherical cap at zero gravity. The drop profile is computed exactly in the same approximation. These results are compared with *Surface evolver* results, showing a surprisingly large range of applicability of first order approximations.

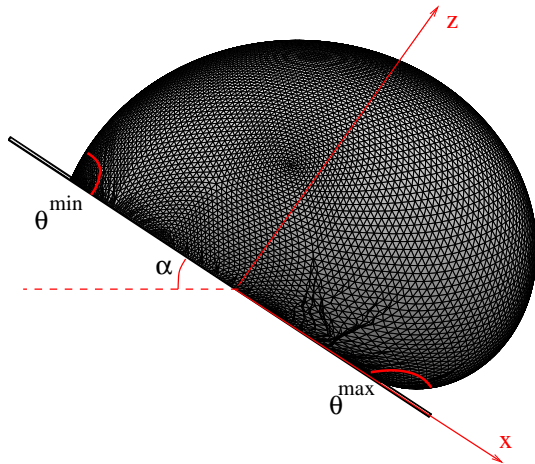


FIG. 1. Water drop on hydrophobic incline at angle $\alpha = 30^\circ$. Volume $V \simeq 42\mu\text{L}$. Pinned base radius $r_0 \simeq 2.0\text{mm}$. Simulated with *Surface Evolver*.

Pinning of a drop on an incline is a subject with a long history, see [12][10] and [1] and references therein. Hysteresis of contact angle and the roll-off angle have attracted renewed attention in recent years, motivated by the search for super-hydrophobic materials. The roll-off angle is often used to characterize the quality of a surface: if it is small, say below 5° , the surface is considered as perfect such as a piece of glass or silica wafer. Small roll-off angles are also observed with super-hydrophobic materials such as the lotus leaf. If the roll-off angle is large, say above 10° , then the surface must be heterogeneous, physically in terms of topographical defects or chemically in terms of various species covering the surface, or for most of the industrial cases, both. Advancing and receding contact angles may be defined as follows (see [11] for background and references): consider a small piece of contact line where the three phases meet. The sum of forces parallel to the solid

surface, per unit length of contact line, is perpendicular to the line and defines the local spreading coefficient $\gamma_{SV} - \gamma_{SL} - \gamma \cos \theta = \gamma (\cos \theta_Y - \cos \theta)$ where θ is the local contact angle and θ_Y is the Young angle implied by the equation. The local contact angle θ is a macroscopic quantity, with smooth variation on the macroscopic scale, because the fluid surface is smooth. The Young angle θ_Y , before averaging, follows the heterogeneity of the solid surface energies $\gamma_{SV} - \gamma_{SL}$ and may vary in a range $\theta_1 \leq \theta_Y \leq \theta_2$. If the local contact angle falls in this range then the piece of contact line will undergo positive and negative spreading coefficients and thus will be pinned. Otherwise it will move to one side or the other, defining advancing and receding contact angles.

This is a simplified picture, notably because it deals with metastability through equilibrium macroscopic notions only, which will be wrong at the nano-scale. One should also distinguish Wenzel states wetting nano-pores from Cassie-Baxter states with air pockets, etc. The advancing and receding angles θ^A and θ^R are defined experimentally. But the basic mechanism should be valid, and should imply the following scenario: a drop is gently deposited on a horizontal substrate; the macroscopic contact line is a circle. Suppose the contact angle is $\theta^R < \theta_0 < \theta^A$. Now tilt the substrate by a small angle α . The contact angle along the contact line becomes a function $\theta(\varphi)$ oscillating around θ_0 and therefore satisfying $\theta^R < \theta(\varphi) < \theta^A$ for all φ . The contact line is pinned everywhere and remains circular. Upon increasing α , depending upon θ_0 , the maximum of $\theta(\varphi)$ will reach θ^A or the minimum will reach θ^R and a corresponding piece of the contact line will move by a finite amount. The remaining piece holds the drop. Upon increasing α further, eventually the remaining piece will be unable to hold the drop, or it will reach its limit θ^R or θ^A and the drop will roll off. Such a scenario with three different transitions was already proposed in [1]. If $\theta_0 = \theta^A$ or θ^R , of course the first stage is skipped, and the circle is deformed as soon as $\alpha > 0$. The importance of the deposition history

was already stressed in [13][6][14].

In this letter we consider the first stage, where the contact line is pinned as a circle of radius r_0 . We denote θ_α^{\max} and θ_α^{\min} the contact angles at the front and at the back of the drop when the tilt angle is α (see Fig. 1). We show, for any B , for small α ,

$$mg \sin \alpha = \gamma r_0 \frac{\pi}{2} \left(\cos \theta_\alpha^{\min} - \cos \theta_\alpha^{\max} \right) + \mathcal{O}(\alpha^3) \quad (1)$$

and for any α , for small B ,

$$mg \sin \alpha = \gamma r_0 \frac{\pi}{2} \left(\cos \theta_\alpha^{\min} - \cos \theta_\alpha^{\max} \right) + \mathcal{O}(B^2) \quad (2)$$

Our derivations are analytic, but a factor $\pi/2$ or very near $\pi/2$ was found previously from numerical solutions using the finite elements method [5] or from experiments [7][8], see Fig. 4 in [8]. We use *Surface evolver* [4] to compare first order approximations and numerically almost exact results.

We start from a sessile drop on a plane horizontal substrate, with three-phase contact-line a circle of radius r_0 . We use cylindrical coordinates (z, r, φ) with origin at the center of the contact-line circle. The hydrostatic pressure just below the drop surface is $p = p_0 - \rho g z$ where p_0 is the pressure at the origin and $z = z(r)$ is the drop profile, obeying the Laplace-Young equation

$$p - p_{\text{atm}} = -2\gamma H = -\gamma \left(\frac{z''}{(1+z'^2)^{3/2}} + \frac{z'}{r(1+z'^2)^{1/2}} \right)$$

where γ is the liquid-air surface tension and H is the mean curvature. The boundary conditions are $z'(0) = 0$, $z(r_0) = 0$. Eliminating the pressure gives

$$p_0 - p_{\text{atm}} = \rho g z - 2\gamma H \quad (3)$$

The parameters r_0 and $p_0 - p_{\text{atm}}$ may be changed in terms of drop volume and macroscopic contact angle θ_0 . This angle depends upon the way the sessile drop was deposited on the substrate, and can be any angle between the receding angle and the advancing angle.

Let us tilt the substrate by an angle α , and assume that the contact line does not move, as discussed above. We keep cylindrical coordinates with z -axis perpendicular to the substrate, so that the hydrostatic pressure is now

$$p = p_0 - \rho g z \cos \alpha + \rho g x \sin \alpha$$

where the x -axis is chosen in the direction of the downward slope. Then (3) becomes

$$p_0 - p_{\text{atm}} = \rho g z \cos \alpha - \rho g x \sin \alpha - 2\gamma H \quad (4)$$

where now $z = z(r, \varphi)$, with partial derivatives denoted $z_r, z_\varphi, z_{rr}, z_{r\varphi}, z_{\varphi\varphi}$, and

$$2H = \left(r^2 (z_r^2 + 1) + z_{\varphi\varphi}^2 \right)^{-3/2} \left[r z_{rr} (z_\varphi^2 + r^2) + \right.$$

$$\left. z_r r^2 (z_r^2 + 1) + 2z_r z_\varphi (z_\varphi - r z_{r\varphi}) + r z_{\varphi\varphi} (z_r^2 + 1) \right] \quad (5)$$

At small tilt or small Bond number the solution to (4) will generally admit a Taylor expansion in a small parameter, and one may attempt to solve (4) order by order. We consider the first order, which corresponds to linearizing (4). We assume that order zero has cylindrical symmetry, so that $z(r, \varphi) = z_0(r) + \alpha z_1(r, \varphi) + \text{higher orders}$, or a similar formula with the Bond number instead of α , and the appropriate z_0 in each case. Inserted into (5) this yields $H = H_0 + \alpha H_1 + \text{higher orders}$ or a similar formula with the Bond number instead of α , with, in any case,

$$2H_1 = (1 + z_0'^2)^{-3/2} z_{1rr} + (1 + z_0'^2)^{-1/2} \frac{z_{1\varphi\varphi}}{r^2} + (1 + z_0'^2)^{-3/2} \frac{z_{1r}}{r} - 3z_0'' z_0' (1 + z_0'^2)^{-5/2} z_{1r} \quad (6)$$

Volume conservation and boundary conditions apply to all orders. In particular,

$$0 = \int_0^{2\pi} d\varphi \int_0^{r_0} dr r z_1(r, \varphi), \quad z_1(r_0, \varphi) = 0 \quad \forall \varphi$$

Small tilt

Here we take for z_0 the solution of (3). The pressure p_0 at the center is even in α , so that $p_0 = p_{00} + \mathcal{O}(\alpha^2)$. Order zero in (4) is (3) now written as

$$p_{00} - p_{\text{atm}} = \rho g z_0 - 2\gamma H_0$$

and the contact angle at order zero is given by $\tan \theta_0 = -z_0'(r_0)$. Order one, the coefficient of α in the Taylor expansion of (4) with $z(r, \varphi) = z_0(r) + \alpha z_1(r, \varphi) + \text{higher orders}$, is

$$0 = \rho g z_1 - \rho g r \cos \varphi - 2\gamma H_1 \quad (7)$$

where the polar angle φ is measured from the downward slope direction. An ansatz for a solution is

$$z_1(r, \varphi) = \tilde{z}_1(r) \cos \varphi, \quad \tilde{z}_1(0) = 0, \quad \tilde{z}_1(r_0) = 0$$

Then using (6) it appears that $\cos \varphi$ cancels out from (7), and $\tilde{z}_1(r)$ is the solution of the ordinary differential equation

$$\frac{\rho g r}{\gamma} = \frac{\rho g \tilde{z}_1}{\gamma} - (1 + z_0'^2)^{-3/2} \tilde{z}_1'' - (1 + z_0'^2)^{-1/2} \frac{\tilde{z}_1}{r^2} + (1 + z_0'^2)^{-3/2} \frac{\tilde{z}_1'}{r} - 3z_0'' z_0' (1 + z_0'^2)^{-5/2} \tilde{z}_1' \quad (8)$$

The contact angle $\theta_\alpha(\varphi)$ obeys

$$\tan \theta_\alpha(\varphi) = -\frac{\partial z}{\partial r}(r_0, \varphi) = \tan \theta_0 - \alpha \tilde{z}_1'(r_0) \cos \varphi + \mathcal{O}(\alpha^2)$$

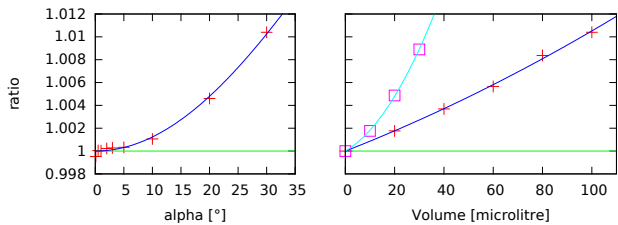


FIG. 2. The ratio (13) function of α (left: 100 μ L droplet, with fit $1 + c \sin^2 \alpha$), and function of drop volume (right: $+(\alpha = 30^\circ)$ and $\square(\alpha = 60^\circ)$, each with fit $1 + aV + bV^2$).

so that

$$\cos \theta_\alpha(\varphi) = \cos \theta_0 + \alpha z_1'(r_0) \sin \theta_0 \cos^2 \theta_0 \cos \varphi + \mathcal{O}(\alpha^2) \quad (9)$$

and

$$\frac{\cos \theta_\alpha(\varphi) - \cos \theta_\alpha^{\max}}{\cos \theta_\alpha^{\min} - \cos \theta_\alpha^{\max}} = \frac{1 - \cos \varphi}{2} + \mathcal{O}(\alpha) \quad (10)$$

to be compared to ElSherbini and Jacobi's formula [7]

$$\frac{\theta_\alpha(\varphi) - \theta_\alpha^{\min}}{\theta_\alpha^{\max} - \theta_\alpha^{\min}} = 2\frac{\varphi^3}{\pi^3} - 3\frac{\varphi^2}{\pi^2} + 1 \quad (11)$$

A comparison is achieved by plotting the right-hand-side of (11) together with the function of φ obtained from the left-hand-side of (11) with $\theta_\alpha(\varphi)$ extracted from (10) without $\mathcal{O}(\alpha)$. The two plots are hardly distinguishable when $\theta_\alpha^{\max} - \theta_\alpha^{\min}$ is small, as considered here.

The total capillary force upon the drop, projected onto the substrate and onto the direction $\varphi = \pi$, upwards along the slope, is:

$$\begin{aligned} F_\gamma &= -\gamma r_0 \int_{-\pi}^{\pi} d\varphi \cos \varphi \cos \theta_\alpha(\varphi) \\ &= \gamma r_0 \frac{\pi}{2} \left(\cos \theta_\alpha^{\min} - \cos \theta_\alpha^{\max} \right) + \mathcal{O}(\alpha^3) \end{aligned} \quad (12)$$

The error is $\mathcal{O}(\alpha^3)$ because the part even in α cancels out when integrating over φ . Equilibrium with gravity implies $F_\gamma = mg \sin \alpha$, giving (1), implying

$$\frac{\gamma r_0 \pi (\cos \theta_\alpha^{\min} - \cos \theta_\alpha^{\max})}{2mg \sin \alpha} = 1 + \mathcal{O}(\alpha^2) \quad \text{as } \alpha \rightarrow 0 \quad (13)$$

Formula (9) can then be written as

$$\cos \theta_\alpha(\varphi) = \cos \theta_0 - \frac{mg \sin \alpha}{\gamma r_0 \pi} \cos \varphi + \mathcal{O}(\alpha^2)$$

We have used *Surface evolver* to compute the ratio (13) numerically for α varying between 0.1° and 30° for a 100 μ L droplet with base radius 6 mm, corresponding to $\theta_0 \simeq 32^\circ$, see Fig. 2 (left). Maximum and minimum contact angles, in the plane of symmetry of the drop, were measured by a quadratic fit with three points nearest

to the contact line. The error on the ratio is inversely proportional to the number of vertices times $\sin \alpha$. For α greater than 5° error bars are too small to be shown. For α smaller than 5° the limiting value 1 or a value derived from the quadratic fit are better. The value 0.9995 for $\alpha = 0.1^\circ$ compared to 1.00003 for $\alpha = 1^\circ$ illustrates the divergence of the error as $\alpha \searrow 0$.

Small Bond number

The Bond number is a dimensionless ratio between gravitation and capillarity, such as $mg/(\gamma r_0)$, but more often in the form $\rho g L^2/\gamma$, where popular choices for the length L are r_0 or $V^{1/3}$ or R , related by the spherical cap formula,

$$V = \pi R^3 \left(\frac{2}{3} - \cos \theta_0 + \frac{1}{3} \cos^3 \theta_0 \right), \quad r_0 = R \sin \theta_0$$

where θ_0 is the contact angle. All Bond numbers generally give the same order of magnitude, but must be specified for quantitative comparisons. Here we choose $B = \rho g R^2/\gamma$ for algebraic simplicity. The drop profile at $g = 0$ is independent of the tilt,

$$z_{00} = \sqrt{R^2 - r^2} - \sqrt{R^2 - r_0^2} \quad (14)$$

and the corresponding curvature, and the pressure at the origin, are

$$H_0 = -\frac{1}{R}, \quad p_{00} = p_{\text{atm}} + \frac{2\gamma}{R} \quad (15)$$

We now assume a Taylor expansion $z(r, \varphi) = z_{00}(r) + Bz_1(r, \varphi) + \mathcal{O}(B^2)$ which inserted into (5) yields

$$H = -\frac{1}{R} + BH_1 + \mathcal{O}(B^2) \quad (16)$$

with H_1 given by (6) with z_{00} instead of z_0 , which using (14) simplifies to

$$2H_1 = (1-t)^{3/2} z_{1rr} + (1-t)^{1/2} \frac{z_{1\varphi\varphi}}{r^2} + (1-t)^{1/2} (1-4t) \frac{z_{1r}}{r} \quad (17)$$

where $t = r^2/R^2$. We then define a dimensionless first order pressure correction p_1 by

$$p_0 - p_{\text{atm}} = \frac{2\gamma}{R} + B \frac{\gamma}{R} p_1 \cos \alpha + \text{higher orders} \quad (18)$$

Order one in equation (4) takes the form

$$p_1 \cos \alpha = \frac{z_{00}}{R} \cos \alpha - \frac{r}{R} \sin \alpha \cos \varphi - 2RH_1 \quad (19)$$

Equation (4) is invariant under $\alpha \rightarrow -\alpha$, $\varphi \rightarrow \pi - \varphi$, one can separate odd and even parts of $z - z_{00}$. Accordingly, at first order, we try the ansatz

$$z_1(r, \varphi) = z_{01}(r) \cos \alpha + z_{11}(r) \sin \alpha \cos \varphi \quad (20)$$

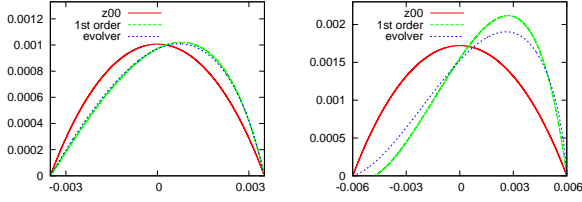


FIG. 3. Drop on 30° incline: spherical cap z_{00} , first order $z_{00} + Bz_{11}$, and *Surface evolver* profiles. Right: volume $100\mu\text{L}$, base radius $r_0 = 6$ mm, Bond number $B = 17.2$. Left: volume $20\mu\text{L}$, base radius $6 \times 0.2^{1/3}$ mm, Bond number $B = 5.89$. Abscissa x along incline, downwards, and ordinate z perpendicular to incline, both in meters.

Since (19) is linear and the two terms in (20) are linearly independent, it yields two independent differential equations where $\cos \alpha$ and $\sin \alpha \cos \varphi$ factor out,

$$p_1 = \frac{z_{00}}{R} - 2RH_{01}, \quad 0 = 2\pi \int_0^{r_0} dr r z_{01}, \quad z_{01}(r_0) = 0 \quad (21)$$

$$0 = -\frac{r}{R} - 2RH_{11}, \quad z_{11}(0) = 0, \quad z_{11}(r_0) = 0 \quad (22)$$

where $2H_{01}$ is (17) for z_{01} instead of z_1 , without the $z_{1\varphi}$ term, and

$$2H_{11} = (1-t)^{3/2} z_{11}'' - (1-t)^{1/2} \frac{z_{11}'}{r^2} + (1-t)^{1/2} (1-4t) \frac{z_{11}'}{r}$$

Like the small tilt case, equations (20)(21)(22) imply (2),

$$\frac{\gamma r_0 \pi (\cos \theta_\alpha^{\min} - \cos \theta_\alpha^{\max})}{2mg \sin \alpha} = 1 + \mathcal{O}(B) \quad \text{as } B \rightarrow 0 \quad (23)$$

We have used *Surface evolver* to compute the ratio (23) numerically for $\alpha = 30^\circ$ and $\alpha = 60^\circ$ as function of volume, when the contact angle at $g = 0$ is $\theta_0 \simeq 32^\circ$, see Fig. 2 (right), where $B = 17.2 \times (V/100)^{(2/3)}$.

Equations (21)(22) can be solved exactly. In equation (22) the change of variable $t = r^2/R^2$ and function $v = rz_{11}/R^2$ leads to

$$(1-t)^{-1/2} = -4(1-t)v'' + 6v' - 2\frac{v}{t}, \quad v(0) = 0, \quad v(t_0) = 0$$

Mathematica gives the solution:

$$v = t(1-t)^{-1/2} C_1 + \frac{1}{3} - \frac{1}{3}(1-t)^{1/2} + \frac{1}{3}t(1-t)^{-1/2} \ln(1 + (1-t)^{1/2}) \quad (24)$$

where C_1 is fixed by $v(t_0) = 0$. Equation (21) was solved in [9]. We give here an equivalent solution:

$$z_{01}'' + r^{-1}(1-t)^{-1}(1-4t)z_{01}' = R^{-2}(1-t)^{-3/2}(z_{00} - Rp_1)$$

or, with $u = z_{01}'r/R$ and $t_0 = r_0^2/R^2$,

$$2u' - \frac{3u}{1-t} = (1-t)^{-1} - ((1-t_0)^{1/2} + p_1)(1-t)^{-3/2}$$

This is a first order linear differential equation which can be solved by the variation of constants method, yielding

$$u(t) = \frac{1}{3}(1-t)^{-3/2} - \frac{1}{3} - \frac{1}{2}((1-t_0)^{1/2} + p_1)t(1-t)^{-3/2}$$

The volume of the drop doesn't vary:

$$0 = 2\pi \int_0^{r_0} dr r z_{01} = -\pi \int_0^{r_0} dr r^2 z_{01}' = -\frac{\pi R^3}{2} \int_0^{t_0} dt u$$

implying

$$p_1 = \frac{\frac{8}{3} - 2t_0 + (1-t_0)^{1/2} \left(\frac{2t_0}{3} - \frac{8}{3} \right)}{2 - t_0 - 2(1-t_0)^{1/2}} \quad (25)$$

Then

$$z_{01}(r) = \int_{r_0}^r d\ell z_{01}'(\ell) = \frac{R}{2} \int_{t_0}^t ds \frac{u(s)}{s} = \frac{R}{2} \left(\frac{I}{3} + J \right) \quad (26)$$

where

$$I = 2(1-t)^{-1/2} - 2(1-t_0)^{-1/2} - 2 \log \left[\frac{1 + (1-t)^{1/2}}{1 + (1-t_0)^{1/2}} \right]$$

$$J = ((1-t_0)^{1/2} + p_1) ((1-t_0)^{-1/2} - (1-t)^{-1/2})$$

Resulting $z = z_{00} + Bz_{01} \cos \alpha + Bz_{11} \sin \alpha \cos \varphi$ with z_{01} given by (26) and $z_{11} = vR^2/r$ given by (24) are shown on Fig. 3 as “first order”, together with the spherical cap z_{00} and the almost exact *Surface evolver* results. The profile with $B = 17.2$, corresponding to the top right points for the ratio on Fig. 2 (left and right figures), is not far from the physical limitation $\theta_\alpha^{\min} = 0$, and the first order approximation in fact gives a small negative value for θ_α^{\min} .

Overhangs

The derivation so far used height functions $z(r, \varphi)$, which excludes overhangs and contact angles larger than $\pi/2$. Yet singularities only occur at contact angles 0 and π , beyond which a fraction of the drop profile would go into $z < 0$ if continued analytically. The laws (1)(2) therefore extend to $0 < \theta^{\min} < \theta^{\max} < \pi$. As for the drop profile, the apparent singularity at $\pi/2$ disappears in polar coordinates with origin at the center of the spherical cap for $B = 0$, angle $\theta \in [0, \theta_0]$ measured from the z -axis and angle $\varphi \in [0, 2\pi]$ as before,

$$\vec{r}(\theta, \varphi) = (R + \delta r(\theta, \varphi)) \vec{e}_r, \quad \delta r(\theta_0, \varphi) = 0$$

New formulas are derived from the old, first in the case $\theta_0 < \pi/2$ using

$$\delta r = Bz_{01} \cos \alpha \cos \theta + Bz_{11} \sin \alpha \cos \theta \cos \varphi$$

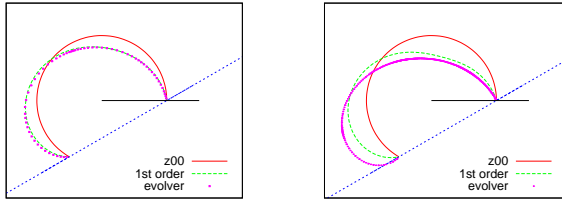


FIG. 4. Drop on 30° hydrophobic incline: spherical cap z_{00} with contact angle $2\pi/3$, first order $z_{00} + Bz_1$ and *Surface evolver* profiles. Left: Bond number $B = 0.5$, corresponding to a volume $V \simeq 25\mu\text{L}$ and base radius $r_0 \simeq 1.7\text{mm}$. Right: $B = 0.8$, corresponding to $V \simeq 51\mu\text{L}$ and $r_0 \simeq 2.1\text{mm}$. The profiles are scaled by a factor r_0^{-1} for comparison.

and $(1 - t_0)^{1/2} = \cos\theta_0$, $(1 - t)^{1/2} = \cos\theta$ and then extended analytically to the whole range of θ with $\theta_0 \in]0, \pi[$, where the cosines can be negative. Results are shown on Fig. 4. One may note that the first order in B overestimates the effect of gravity in the hydrophilic case but underestimates in the hydrophobic case.

The scope of the present study is the physical range $0 \leq \theta^R \leq \theta_\alpha^{\min} \leq \theta_\alpha^{\max} \leq \theta^A \leq \pi$. It is remarkable that the first order approximation is typically within 1% of the almost exact *Surface evolver* result in this full range, whatever the advancing and receding contact angles θ^A and θ^R . The exact solution of the linearized Laplace-Young equation given in the present work together with the simple formulas (1)(2) should therefore be valuable.

This research was partially funded by the Inter-University Attraction Poles Programme (IAP 7/38 MicroMAST) of the Belgian Science Policy Office. The authors also thank FNRS and Région Wallonne for partial support.

-
- [1] V. Berejnov, R. E. Thorne: *Effect of transient pinning on stability of drops sitting on an inclined plane*. Phys. Rev. E **75**, 066308 (2007).
 - [2] J. Berthier: *Microdrops and digital microfluidics*. Elsevier, second edition (2013).
 - [3] J. Berthier, K. Brakke: *The physics of microdroplets*. Scrivener-Wiley (2012).
 - [4] K. Brakke: *Surface Evolver Manual*. Susquehanna University (2013).
 - [5] R. A. Brown, F. M. Orr, Jr., L. E. Scriven: *Static Drop on an Inclined Plate: Analysis by the Finite Element Method*. J. Colloid Interface Sci. **73**, 76-87 (1980).
 - [6] T.-H. Chou, S.-J. Hong, Y.-J. Sheng, H.-K. Tsao: *Drops sitting on a tilted plate: Receding and advancing pinning*. Langmuir **28**, 5158-5166 (2012).
 - [7] A.I. ElSherbini, A.M. Jacobi: *Liquid drops on vertical and inclined surfaces I. An experimental study of drop geometry*. J. Colloid Interface Sci. **273**, 556-565 (2004).
 - [8] A.I. ElSherbini, A.M. Jacobi: *Retention forces and contact angles for critical liquid drops on non-horizontal surfaces*. J. Colloid Interface Sci. **299**, 841 (2006).
 - [9] A.H. Fatollahi: *On the shape of a lightweight drop on a horizontal plane*. Phys. Scr. **85** (2012) 045401 (6pp)
 - [10] Y. I. Frenkel: *On the behavior of liquid drops on a solid surface 1. The sliding of drops on an inclined surface*. Zh. Eksp. Teor. Fiz. **18**, 659 (1948). Translated by V. Berejnov: <http://xxx.lanl.gov/abs/physics/0503051>
 - [11] P.-G. de Gennes, F. Brochard-Wyart, D. Quéré: *Capillarity and Wetting Phenomena: Drops, Bubbles, Pearls, Waves*. Springer-Verlag (2003).
 - [12] G. Macdougall, C. Ockrent: *Surface energy relations in liquid/solid systems*. Proc. R. Soc. London, Ser. A **180**, 151-173 (1942).
 - [13] M. Musterd, V. van Steijn, C. R. Kleijn, and M. T. Kreutzer: *Droplets on inclined plates: Local and global hysteresis of pinned capillary surfaces*. Phys. Rev. Lett. **113**, 066104 (2014).
 - [14] J. A. White, M. J. Santos, M. A. Rodríguez-Valverde, S. Velasco: *Numerical Study of the Most Stable Contact Angle of Drops on Tilted Surfaces*. Langmuir **31**, 5326-5332 (2015).